

# Suspension-Expansion of Bone Marrow Results in Small Mesenchymal Stem Cells Exhibiting Increased Transpulmonary Passage Following Intravenous Administration

Andrea Zanetti, DVM, PhD,<sup>1</sup> Michelle Grata, BS,<sup>1</sup> Emily B. Etling, BS,<sup>1</sup> Regeant Panday, BS,<sup>1</sup> Flordeliza S. Villanueva, MD,<sup>1,2</sup> and Catalin Toma, MD<sup>1,2</sup>

Mesenchymal stem cells (MSCs) have been extensively explored in a variety of regenerative medicine applications. The relatively large size of MSCs expanded in tissue culture flasks leads to retention in the microcirculation of the lungs following intravenous delivery, reducing their capacity to reach target sites. We explored whether the expansion of whole marrow in suspension cultures would yield smaller MSCs with increased capacity to traverse the pulmonary microcirculation compared with traditional monolayer cultures. We tested this hypothesis using rat marrow in a suspension bioreactor culture with fibronectin-coated microcarriers, leading to sustained expansion of both the microbead-adherent cells, as well as of a nonadherent cell fraction. Magnetic depletion of CD45<sup>+</sup> cells from the bioreactor cultures after 5 weeks led to a highly enriched CD73<sup>+</sup>/CD90<sup>+</sup>/CD105<sup>+</sup> MSC population. The bioreactor-grown MSCs were significantly smaller than parallel monolayer MSCs ( $15.1 \pm 0.9 \mu\text{m}$  vs.  $18.5 \pm 2.3 \mu\text{m}$  diameter,  $p < 0.05$ ). When fluorescently labeled bioreactor-grown MSCs were intravenously injected into rats, the peak cell concentration in the arterial circulation was an order of magnitude higher than similarly delivered monolayer-grown MSCs ( $94.8 \pm 29.6$  vs.  $8.2 \pm 5.6/10^6$  nucleated blood cells, respectively,  $p < 0.05$ ). At 24 h after intravenous injection of the *LacZ*-labeled bioreactor-grown MSCs, there was a significant threefold decrease in the *LacZ*-labeled MSCs trapped in the lungs, with a significant increase in the cells reaching the spleen and liver in comparison to their monolayer MSC counterparts. Bioreactor-grown whole marrow cell cultures yielded smaller MSCs with increased capacity to traverse the pulmonary microcirculation compared with traditionally expanded monolayer MSCs. This may significantly improve the capacity and efficiency of these cells to home to injury sites downstream of the lungs.

## Introduction

MESENCHYMAL STEM CELLS (MSCs) have been extensively explored for their tissue repair and immunomodulating properties in a variety of disease processes.<sup>1</sup> Administration of MSCs has recently been approved outside the United States for the treatment of refractory graft versus host disease.<sup>2,3</sup> However, clinical studies looking at the intravenous route of administration for other applications, including cardiovascular and pulmonary conditions, have yielded only modest improvements to date.<sup>4-6</sup>

One of the potential problems with the intravenous administration culture-expanded MSCs is their poor capacity to traverse the pulmonary microcirculation.<sup>7-10</sup> Studies have demonstrated that a small number of MSCs subsequently redistribute to other organs following this initial lung en-

trapment.<sup>9</sup> Using intravital microscopy, we have previously demonstrated that when delivered in the bloodstream, the vast majority of the MSCs become entrapped at the precapillary level, leading to increased cell demise.<sup>11</sup> Moreover, this could potentially lead to local flow cessation and detrimental microischemia<sup>11</sup> or inflammation.<sup>12</sup> The data demonstrated that this behavior is mainly explained by the large size of these cells (averaging  $20 \mu\text{m}$  in diameter), which impedes their individual passage through the microcirculation.<sup>11</sup>

Thus, engineering smaller MSCs with an improved rheological profile could result in enhanced therapeutic potential.<sup>11</sup> MSCs are isolated from bone marrow aspirates by selectively enriching cells adhered to tissue culture substrates,<sup>13</sup> leading to a relatively homogenous MSC population by passages 3-4.<sup>13,14</sup> This represents an environment

<sup>1</sup>Heart and Vascular Institute, University of Pittsburgh and University of Pittsburgh Medical Center, Pittsburgh, Pennsylvania.

<sup>2</sup>The McGowan Center for Regenerative Medicine, University of Pittsburgh, Pittsburgh, Pennsylvania.

markedly different from the native bone marrow, where there is constant paracrine crosstalk between different cell types.<sup>15,16</sup> Suspension culture expansion systems have been developed<sup>15,17</sup> that offer an alternative, where MSC expansion occurs in parallel with active hematopoiesis. It has been suggested that the MSCs generated in these systems are smaller in size, and have properties resembling naive bone marrow MSCs.<sup>15</sup>

Based on this information, in the present study we characterized the expansion of MSCs in whole marrow suspension cultures, demonstrating the feasibility of this approach in producing smaller MSCs. Subsequently, we investigated the biodistribution of these bioreactor-grown MSCs following intravenous administration in rats, demonstrating their increased capacity to traverse the lung microcirculation relative to MSCs conventionally expanded.

## Materials and Methods

All animal procedures were approved by the Institutional Animal Use and Care Committee at the University of Pittsburgh.

### Cell culture

Rat bone marrow was obtained from adult male Sprague Dawley rats weighing 150–300 g (Jackson Laboratory, Bar Harbor, ME). The femurs and tibias were harvested under

sterile conditions. The articular surfaces of the bones were removed, and the marrows were forcefully flushed with phosphate buffered saline (PBS; Lonza, Allendale, NJ). Initial pilot experiments were done with bone marrow mononuclear cells obtained after Ficoll (GE Healthcare Life Sciences, Uppsala, Sweden) separation (density:  $10^6$  cells/mL) and cultured using the conditions described below. After data for the pilot studies were reviewed, in subsequent experiments, the entire bone marrow population was either plated on regular tissue culture flasks (monolayer cultures) or loaded in 25-mL Bellco<sup>®</sup> glass bioreactors (bioreactor cultures). These bioreactors have a magnetically driven impeller with a vertical axis of rotation at speed of 108 rpm that prevented sedimentation of the cells (Fig. 1A). The initial cell density was  $10^6$  cells/cm<sup>2</sup> in T75 flasks for the monolayer cultures and  $10^7$  cells/mL plus fibronectin-coated Cultispher<sup>®</sup> G gelatin beads (Sigma-Aldrich, St. Louis, MO) at 75 mg dry weight/13 mL media for the bioreactors. The impeller was placed close to the bottom of the bioreactor to ensure adequate stirring and prevent bead sedimentation. Both culture conditions (monolayer and bioreactor) were maintained in humidified 37°C and 5% CO<sub>2</sub> incubators. The media used was  $\alpha$ -minimum essential medium ( $\alpha$ -MEM) (Gibco, Grand Island, NY) supplemented with 20% fetal bovine serum (FBS, cat# D1100; Atlanta Biologicals, Lawrenceville, GA), 4 mM L-glutamine

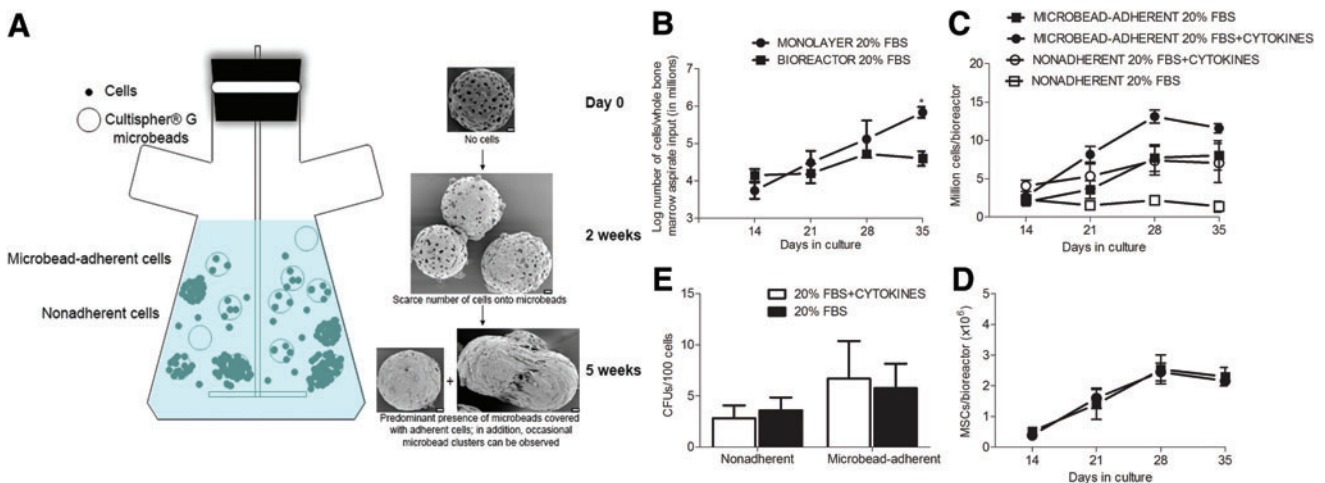


**FIG. 1.** Suspension bioreactor expansion of bone marrow cells. (A) The Bellco<sup>®</sup> bioreactor system used for the whole bone marrow cultures in suspension in the presence of fibronectin-coated microbead carriers (Cultispher<sup>®</sup>). Throughout the culture period, the bioreactors contained both a microbead-adherent as well as a nonadherent cell population. On scanning electron microscopy examination scarce number of cells were observed adherent to the microbeads after 2 weeks of culture, while after 5 weeks the microbeads were coated with cells. Occasional microbead clusters were also observed. Scale bar, 20  $\mu$ m. (B) The cell expansion curves of parallel cultures of whole bone marrow aspirates in bioreactors (square) and monolayer (circle) conditions in 20% fetal bovine serum (FBS) medium. A significant difference in the number of cells/million cells of whole bone marrow aspirate input between the two culture conditions was observed after 35 days of culture ( $p < 0.05$ ). (C) The growth curve for the microbead adherent (open symbols) and nonadherent (closed symbols) cell fractions in regular mesenchymal stem cells (MSCs) media (20% FBS minimum essential medium [MEM], squares) or media supplemented with cytokines (interleukin-3 [IL3], interleukin-6 [IL6], and stem cell factor [SCF], circles); no statistical differences were noted between the two culture conditions. (D) The colony forming unit assay (CFU) forming capacity (per 100 cells) of the nonadherent and the adherent cells fractions, indicating similar proportion of MSCs in both culture conditions. The presence of MSCs in the nonadherent fraction allowed for culture growth simply by adding new beads and media. (E) The expansion of microbead-adherent MSCs (defined as CD45<sup>-</sup>/CD90<sup>+</sup>/CD73<sup>+</sup> by multicolor flow cytometry) over time in bioreactors in regular MSCs media (20% FBS MEM, squares) or media supplemented with cytokines (IL3, IL6, and SCF, circles); no statistical differences were noted between the two culture conditions. Color images available online at [www.liebertpub.com/tec](http://www.liebertpub.com/tec)

(Sigma-Aldrich) and 1% penicillin/streptomycin (Lonza). Additionally, for the bioreactors we also compared the referred medium (20% FBS) with parallel cultures of the same medium enriched with recombinant rat cytokines (referred to in this study as 20% FBS+cytokines, comprised of stem cell factor, 40 ng/mL; interleukin-3 [IL3], 10 ng/mL; and interleukin-6 [IL6], 10 ng/mL), which were previously reported to be necessary to maintain human bone marrow suspension cultures.<sup>18</sup> These parallel cultures were initially maintained with 20% FBS+cytokines for the first 3 days. Subsequently, the medium was diluted 1:5 from the initial cytokine concentration and hydrocortisone ( $10^{-6}$  M) was added.<sup>18</sup>

#### *Growth profiling of bioreactor-expanded cells*

Characterization of cell growth on microbeads began 2 weeks postinitial bioreactor cell loading and continued on a weekly basis thereafter. In addition, gelatin beads from 3 mL of media were digested using dyspase<sup>®</sup> (1 mg/mL; Stem cells Technologies, Vancouver, Canada) to release the microbead-adherent cells, which were then counted. At each time point, cell feeding was done by fully replacing the bioreactor media while retaining the nonadherent cells by centrifugation. Fresh CultiSpher beads were also added to the bioreactors to replace the ones removed for cell analysis. Subsequent cell counts were corrected for these repeated dilutions. Cell concentration was measured with an automated cell counter device (Countless<sup>®</sup>; Invitrogen, Carlsbad, CA).

#### *Colony forming unit assay*

After 5 weeks of culture, bioreactor-expanded MSCs (both microbead-adherent and the nonadherent fractions) were dyspase digested. Then, the cells were plated at density of  $1 \times 10^3$  cells/well in six-well plates (BD Falcon<sup>®</sup>; BD BioSciences, San Jose, CA) to assess the colony forming units (CFUs) potential of MSCs. At the end of week 2, the cells were stained with crystal violet (Lonza) and macroscopically visible colonies (>30 cells) were counted.

#### *Multipotential differentiation of bioreactor-expanded MSCs*

Following dyspase digestion of the beads at the end of the cell culture experiments (5 weeks), the bioreactor cells were plated in six-well plates (BD Falcon; BD BioSciences) in parallel to monolayer MSCs (passage 4). After achieving cell confluence, the maintenance media in both plates were switched to either adipogenic (DMEM-High glucose<sup>®</sup>; Lonza, supplemented with 20% FBS, 1% L-glutamine, 1% penicillin/streptomycin, 1  $\mu$ M dexamethasone, 1  $\mu$ M indomethacin, 500  $\mu$ M 3-isobutyl-1-methylxanthine [IBMX], and 10  $\mu$ g/mL human recombinant insulin) or osteogenic (Dulbecco's modified Eagle's medium [DMEM], 10% FBS, 2 mM L-glutamine, 100 U/mL penicillin, 100  $\mu$ g/mL streptomycin, 20 mM  $\beta$ -glycerol phosphate, 50  $\mu$ M ascorbic acid, and 100 nM dexamethasone) induction media. Alizarin red (Lifeline Cell Technology, Frederick, MD) and Oil Red O (Lonza) stains were used to assess the osteogenic and adipogenic differentiation of the cells after 14 and 18 days of culture, respectively, as previously described.<sup>14</sup>

#### *Scanning electron microscopy*

For scanning electron microscopy of beads only and beads containing cells at 2 and 5 weeks of culture, the beads were fixed in 2.5% glutaraldehyde for 1 h, washed with PBS, and then postfixed in aqueous 1% OsO<sub>4</sub> for 30 min before consecutive washes in PBS. Samples were then dehydrated through a graded ethanol series (30–100%) and washed with absolute ethanol before drying in hexamethyldisilazane solution. Finally, samples were sputter coated with 6 nm of gold/palladium (Cressington Auto 108, Cressington, United Kingdom). Imaging was performed on a JEOL JSM-6335F scanning electron microscope (Jeol, Inc., Peabody, MA) at 3 kV with the SEI detector.

#### *Immunophenotyping of bioreactor MSCs*

Phenotypic characterization of the cells was performed using a three-color FACSCalibur instrument (Beckton Dickinson, Franklin Lakes, NJ). The following antibodies were used: mouse monoclonal anti-rat CD73 (clone 5F/B9; BD Bioscience), mouse monoclonal PE anti-rat CD45 (clone OX-1; BD Bioscience), goat polyclonal anti-endoglin CD105 (clone M-20; Santa Cruz Biotechnology, Dallas, TX), mouse monoclonal PerCP-conjugated anti-CD90 (clone Thy-1.1; Santa Cruz Biotechnology). The nonconjugated antibodies (anti-CD73 and CD105) were first conjugated with fluorescein-X (FAM-X) using a SureLink Fluorescein-X labeling kit (KPL, Gaithersburg, MD), according to the manufacturer's instructions. Appropriate FAM-X-conjugated isotype controls (mouse IgG) were created as well. All antibodies were used at dilution ranges from 1:25 to 1:100. Cells were first incubated with mouse IgG at 1:100 dilution to block nonspecific antibody binding, followed by the addition of the labeled antibodies. For the CD105 analysis, cells were first fixed with 4% paraformaldehyde for 10 min, followed by the blocking step. After 20–40 min of incubation at 4°C with primary antibodies, cells were washed and flow analysis was performed. Events were appropriately gated to exclude cellular debris. To quantify the MSC population in the cell culture experiments, three-color flow analysis on the whole bioreactor adherent cell population was performed, with MSCs defined as CD45<sup>-</sup>/CD73<sup>+</sup>/CD90<sup>+</sup> events.

#### *MSC isolation from bioreactor cultures*

Given that the majority of the CD45<sup>-</sup> cells in the bioreactors were phenotypically consistent with MSCs (i.e., CD73/90/105 positive), a CD45<sup>+</sup> cell depletion approach was employed to enrich the MSCs for the subsequent *in vivo* experiments. Briefly, at the end of the culture expansion experiment, bioreactor outputs (both microbead-adherent and the nonadherent fractions) were first dyspase digested. Then, the cells were washed with calcium-free PBS and incubated with mouse IgG at 1:100 dilution to prevent nonspecific antibody binding, followed by anti-CD45 PE-conjugated (clone OX1; BD Bioscience) monoclonal antibody at 1:100. Anti-PE magnetic microbeads (Miltenyi Biotec, Auburn, CA) were then added at a ratio of 20  $\mu$ L of anti-PE microbeads/ $10^7$  cells, followed by 20 min incubation at 4°C. The bioreactor-expanded cells were then eluted through a MACS<sup>®</sup> LD Column (Miltenyi Biotec) placed in a permanent magnet with retention of the CD45<sup>+</sup>/PE-labeled cells inside the column.

Eluted cells (referred to hereafter as bioreactor MSCs) were then characterized by flow cytometry. Before *in vivo* experiments, the bioreactor MSCs were recovered from the prolonged exposure to calcium-free medium by overnight culture in tissue culture flasks (density:  $1.2 \times 10^6$  cells/T175 cm<sup>2</sup>).

#### Measurement of cell size

Cell size was measured using the Countless device (Invitrogen), which allows for optical measurement of the cell's diameter. However, this method is not suited for measuring the size of a particular cell type (such as MSCs) in a mixed cell population. This is particularly relevant in the native bone marrow, where the MSCs are very rare and difficult to physically isolate. Forward side scatter (FSC) in flow cytometry has been shown to linearly correlate with cell size.<sup>19</sup> We, therefore, used the median FSC of the CD45<sup>-</sup>/CD73<sup>+</sup>/CD90<sup>+</sup> cells in these mixed suspension cultures as an alternate way to compare MSCs size between different conditions (native marrow, monolayer and bioreactor MSCs following MACSs separation at baseline and after 6–8 weeks in culture).

#### *In vivo* experiments assessing transpulmonary MSC passage

Experiments were designed to compare the relative ability of bioreactor MSCs and their monolayer counterparts to traverse the lung microcirculation. In these experiments, male Sprague Dawley rats (200–300 g,  $n=6$ /MSC culture condition) were used. Briefly, anesthesia was induced with 3% isoflurane, which was then reduced to 2% when deep breathing and no palpebral or toe pinch reflexes were evident. At this point, a 24-G cannula was placed in the right internal jugular vein for MSC administration and in the contralateral carotid artery for acute blood collection. In both the acute and the chronic experiments, bioreactor MSCs were compared with monolayer MSCs expanded in parallel for the same duration of time (6–8 weeks) in a paired fashion.

In the acute biodistribution experiments, rat (bioreactor and monolayer) MSCs were fluorescently-labeled (1  $\mu$ M of CellTracker<sup>®</sup>-green CMFDA for 30–60 min; Invitrogen) and trypsinized. A bolus of  $1-1.5 \times 10^6$  fluorescent-labeled MSCs in 1 mL Hank's balanced salt solution (HBSS; Lonza) with 100 U/mL of heparin, was then injected over 30 s through the jugular vein cannula. To quantify transpulmonary passage of MSCs, arterial blood samples (0.4 mL) were obtained from the carotid artery cannula at time point 0 (baseline-preinjection) and at predefined intervals up to 15 min postinjection, followed by euthanasia using isoflurane overdose. The arterial samples were subjected to red blood cell lysis (BD Pharm Lyse<sup>™</sup>; BD BioSciences) followed by flow cytometry analysis (up to  $1 \times 10^6$  events/sample) to detect MSCs. The gates were rigorously set to exclude autofluorescent events. Only events clearly positive in the FL1 (fluorescein) channel were counted and normalized to total nucleated blood cells as well as the actual number of injected MSCs. No events were detected in any of the samples at time 0 (preinjection).

In the chronic biodistribution experiments, cells were labeled with an adenoviral vector carrying a *LacZ* gene, supplied by the University of Pittsburgh Vector Core Facility, 12 h before *in vivo* administration. Transfection took place at *LacZ* concentration of 100 multiplicity of infection

in 2% FBS  $\alpha$ -MEM medium. On the surgery day, the MSCs were also fluorescently labeled with CMFDA. A bolus of *LacZ*<sup>+</sup>/CMFDA<sup>+</sup> cells ( $1.4 \times 10^6 \pm 3.4 \times 10^5$  cells/mL) re-suspended in 1 mL HBSS with 100 U/mL of heparin were injected over 30 s through the jugular vein cannula, followed by a 1 mL HBSS flush, removal of the cannula, and closure of the surgical wound. The animals were allowed to recover and transferred to their cages. Postoperatively, buprenorphine (0.25 mg/kg) was subcutaneously administered for pain control. Twenty-four hours post-MSD delivery, the rats were euthanized by isoflurane overdose, and histology and whole organ  $\beta$ -galactosidase activity were used to assess the cell burden in the rats' lungs, spleens, and livers.

#### Histological analysis

Fresh specimens were frozen in Tissue-Tek O.C.T. compound (Sakura, Torrance, CA) and sectioned. Frozen lung sections were also subsequently fixed in 10% formalin and stained in 0.5 mg/mL X-gal solution (HistoMark<sup>®</sup>; KPL, Gaithersburg, MD) overnight to visualize *LacZ*<sup>+</sup> MSCs 24 h postdelivery. Images were taken at 4 $\times$  and 10 $\times$  under an Olympus IX81 inverted fluorescence microscope (Olympus Corp., Center Valley, PA). Two-dimensional images of each specimen were stacked together with the CS6 Adobe Photoshop<sup>®</sup> to facilitate visualization of fluorescent-labeled cells in whole reconstructed lungs, spleen, and liver sections; and *LacZ*<sup>+</sup> cells in the lungs.

#### $\beta$ -Galactosidase activity

The overall  $\beta$ -galactosidase activity was used to quantify the content of the *LacZ*-labeled MSCs in lungs, spleens, and livers of the animals in the 24 h biodistribution studies. Briefly, the organs were homogenized with 1 mL of reporter lysis buffer (Promega<sup>®</sup>, Madison, WI)/0.5 g of tissue and centrifuged for 10 min at 12,000 g. The supernatant was then used to measure  $\beta$ -galactosidase activity with the  $\beta$ -Glo assay solution (Promega) after 1 h of incubation at room temperature.<sup>20</sup> The relative light units (RLUs) were measured with a luminometer (PerkinElmer, Boston, MA). The data ( $\beta$ -galactosidase activity/gram of tissue) is represented as absolute RLU values within each organ and culture condition and as a ratio of the RLU in the spleens and livers relative to the lungs. The  $\beta$ -galactosidase enzyme activity in three uninjected rats was also measured in each organ and the average of these results was used as a baseline to subtract endogenous  $\beta$ -galactosidase activity from rats injected with *LacZ*<sup>+</sup> MSCs.

#### Statistical analysis

Data are reported as mean  $\pm$  standard error of mean. For direct comparisons between bioreactor MSCs and monolayer MSCs, a Student's *t*-test was used. For multiple comparisons, an ANOVA test was used followed by a Tukey's *post hoc* testing. Prism 5 (GraphPad Software) was used for statistic comparisons and  $p < 0.05$  was considered significant in all comparisons.

## Results

### Bioreactor expansion of MSCs

Whole rat bone marrow suspension cultures were initially attempted in Bellco bioreactors at the minimum necessary rotating speed to prevent cell sedimentation (40 rpm) using

either 20% FBS or 20% FBS+cytokines, as previously described for human cells.<sup>17,18</sup> The input for these pilot cultures was the mononuclear cellular fraction obtained following Ficoll density gradient centrifugation of the bone marrow aspirates. While notable cell growth was initially observed, the cell number abruptly declined after 2 weeks (data not shown). In these cultures, the number of CFU (used as surrogate for MSCs) increased from  $2.2 \pm 0.6/10^5$  cells at time point 0 to  $21.6 \pm 5.6$  CFUs/ $10^5$  cells (10-fold in 20% FBS) or  $8.6 \pm 4.4$  CFUs/ $10^5$  cells (4-fold in 20% FBS+cytokines) after 2 weeks. This modest MSC expansion was accompanied, however, by significant cell clumping and ultimately complete demise of the suspension cultures by week 3 (data not shown).

However, when fibronectin-coated gelatin microcarriers were added as a substrate in the cultures, robust and sustained cell growth was obtained. These bioreactors contained both microbead-adherent and nonadherent cells (Fig. 1A). Ultrastructural analysis of naked microbeads at the beginning of this experiment (day 0, Fig. 1A) revealed porous beads ranging in diameter from 30 to 210  $\mu\text{m}$  (average  $118.4 \pm 52.4$   $\mu\text{m}$ ,  $n=16$ ) and pore size ranging from 3 to 77  $\mu\text{m}$  (average  $12.5 \pm 13.8$   $\mu\text{m}$ ,  $n=27$ ). At 2 weeks, the

microbeads had few cells on their surface. After 5 weeks of culture, cell coverage of the microbeads had expanded significantly, as indicated by the reduction in visible pores (Fig. 1A). In addition, occasional microbead clusters covered with adherent cells were also later observed (Fig. 1A).

The bioreactor cultures were expanded simply by periodically adding medium and new microbeads to replace the ones used for cell analysis, without actual dissociation and traditional passaging of the cells. Our initial testing did not reveal any growth advantage for the mononuclear cell fraction over unfractionated marrow in these bioreactors (data not shown). Therefore, the latter was used for subsequent experiments. With this new bioreactor setup, cell counts abruptly dropped in the first week, likely due to the disappearance of adult blood cells (mostly erythrocytes and platelets) and repeated media changes. However, after 1–2 weeks of culture, a sustained growth phase followed (Fig. 1B, C). The nonadherent fraction was  $32.7\% \pm 8.9\%$  of the total cell count for the cytokine supplemented media versus  $7.4\% \pm 4.0\%$  for the regular media ( $n=4-6$ ,  $p=0.12$ , Fig. 1C). Although cell growth was numerically higher in the cytokine-supplemented media, compared with regular media, no statistically significant differences were observed (Fig. 1C). A

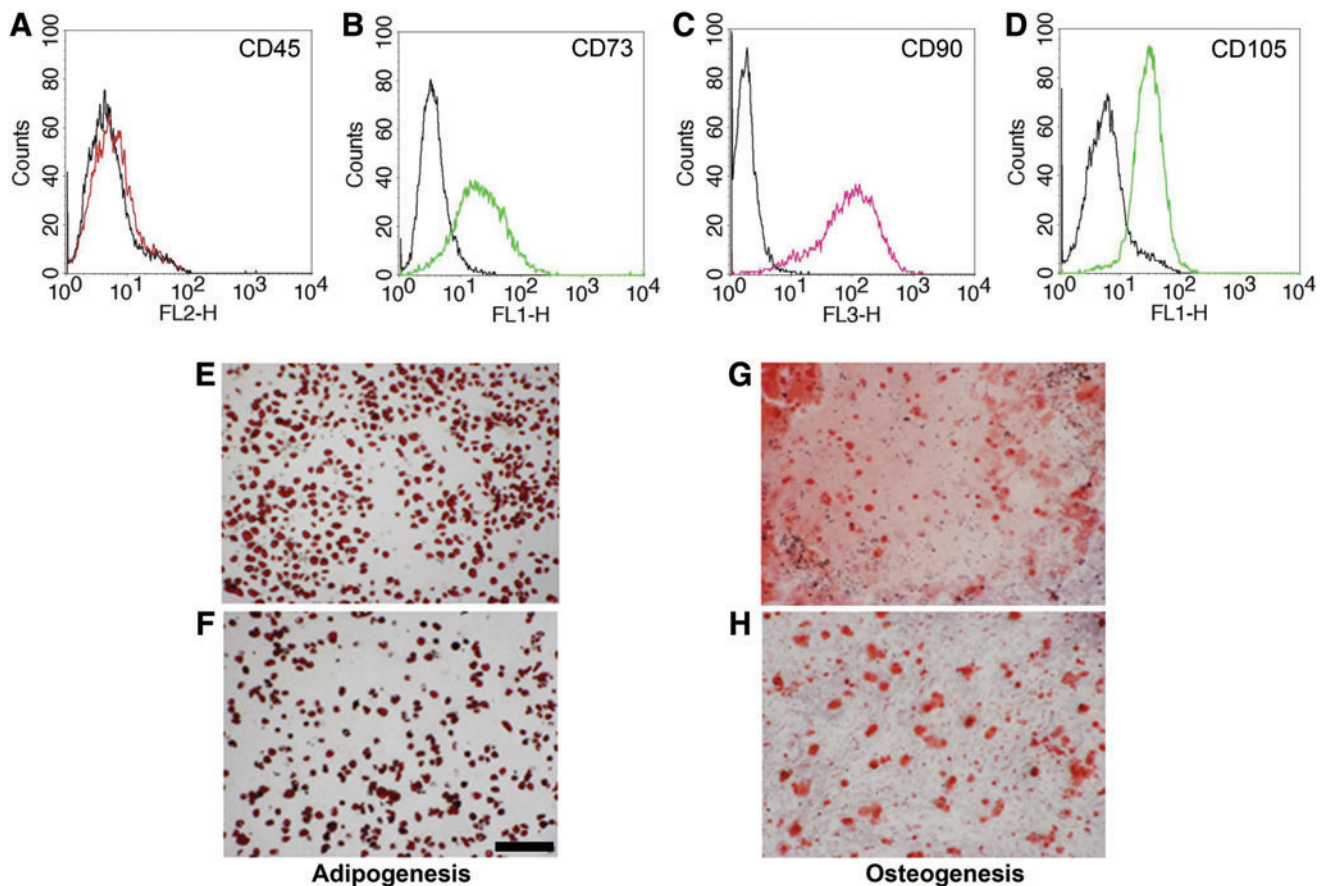


**FIG. 2.** Characterization of the bioreactor-expanded MSCs. Following negative depletion using the CD45<sup>+</sup> MACS<sup>®</sup> column, the remaining cells are as expected CD45 (red) negative (A), and positive for CD73 (green) (B), CD90 (pink) (C), and CD105 (green) (D), consistent with the accepted phenotypic definition of MSCs. The solid black histograms represent the isotype controls for each antibody. Likewise, adherent cells isolated from the bioreactors (E, G) displayed multilineage potential (adipogenic and osteogenic) similar to parallel monolayer cultures (F, H). Scale bar, 100  $\mu\text{m}$ . Color images available online at [www.liebertpub.com/tec](http://www.liebertpub.com/tec)

growth advantage was significant after 35 days for the monolayer cultures versus bioreactor-expanded cells in 20% FBS ( $5.83 \pm 0.14$  million cells/million cells of whole bone marrow aspirate input versus  $4.59 \pm 0.19$  million cells/million cells of whole bone marrow aspirate input  $n=6$ ,  $p < 0.05$ , Fig. 1B).

Unlike the pure suspension cultures (i.e., without microbeads), effective expansion of the MSC population, defined as  $CD45^-/CD73^+/CD90^+$  cells, was obtained in the microbead-containing bioreactors (Fig. 1D). MSC expansion occurred in parallel to the expansion of additional  $CD45^+$  leukocytes, suggestive of active hematopoiesis. Cells isolated from both the microbead-adherent and the nonadherent fractions at 5 weeks were able to form fibroblast-like colonies when plated (Fig. 1E). There was no statistical difference in the total number of MSCs as detected by flow cytometry or the number of CFU-Fs between the regular (20% FBS) and the cytokine-supplemented me-

dia (Fig. 1D, E). Consequently, the latter medium (20% FBS without cytokine supplementation) was used in all subsequent experiments.<sup>21</sup>

Magnetic  $CD45^-$  depletion from bioreactors led to the isolation of a highly enriched MSC fraction, with the majority of the cells being  $CD45^-$  and  $CD73^+/CD90^+/CD105^+$  (Fig. 2A–D). MSC differentiation assays showed that like their monolayer counterparts (Fig. 2F, H), the bioreactor-expanded MSCs (Fig. 2E, G) displayed similar Oil Red O and Alizarin Red staining (Fig. 2F, H).

#### Biophysical properties of the bioreactor-expanded MSCs

An important observation resulting from our experiments is that MSCs undergo a rapid growth in size in culture. FSC in flow cytometry can be used to measure relative cell size. The rare native MSCs in the input bone marrow fraction (defined as

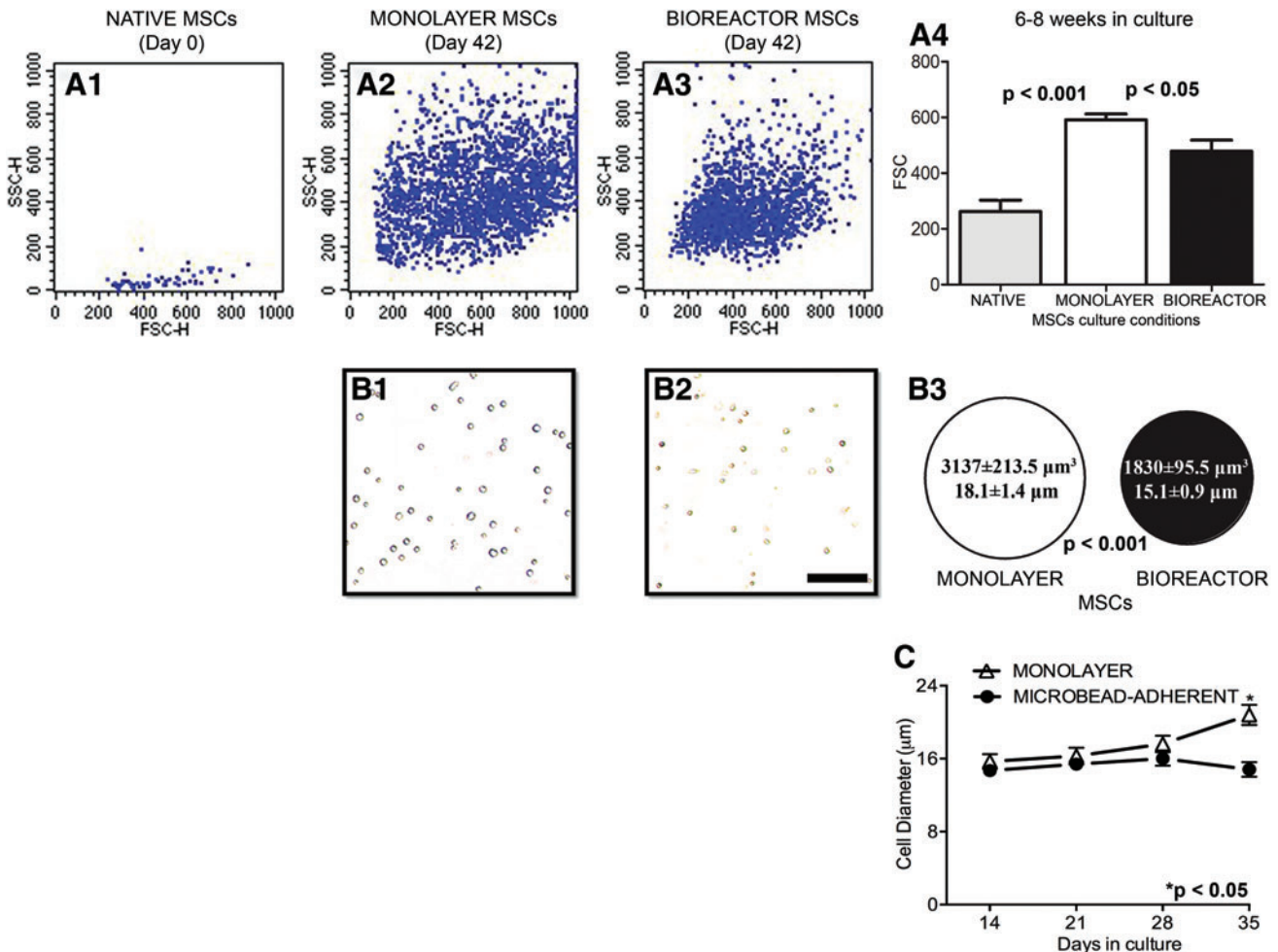


**FIG. 3.** MSCs grow in size in culture. Using the median forward scatter (FSC) as a surrogate for cell size, the rare native MSCs present in freshly isolated rat bone marrow (i.e., the  $CD45^-/CD73^+/CD90^+$  gated fraction, representative flow profile in **A1**) appeared much smaller than the ones expanded in culture under both conditions (**A2**, **A3**,  $p < 0.01$ ). After 6–8 weeks in culture monolayer-expanded MSCs (**A2**) were significantly larger than MSCs expanded in parallel in bioreactor (**A3**, average FSC data in **A4**). This was confirmed by direct measurement of cell size following MACSs bioreactor cell separation using an automated cell counter (representative photomicrographs from monolayer and suspension MSCs in **B1** and **B2**, respectively, and summary data in **B3**). The apparent increase in cell size over time of the mixed cell population present in bioreactors and monolayer conditions is illustrated in (**C**),  $p < 0.05$  or  $0.001$  as indicated. Scale bar, 100  $\mu\text{m}$ . Color images available online at [www.liebertpub.com/tec](http://www.liebertpub.com/tec)

CD45<sup>-</sup>/CD73<sup>+</sup>/CD90<sup>+</sup> cells by 3color flow analysis) had a markedly reduced FSC profile compared with monolayer-cultured cells (Fig. 3A1, A3,  $p < 0.01$ ). MSCs cultured in both monolayer and bioreactor conditions also grew in size, however, after 6–8 weeks in culture, the FSC of the monolayer-expanded cells was significantly higher than that of the bioreactor counterparts ( $591.5 \pm 39.7$  FSC vs.  $478.3 \pm 39.7$  FSC respectively,  $p < 0.05$ , Fig. 3A2–A4), suggesting a smaller size for the later. This was confirmed by direct optical measurements of cell size: after 6–8 weeks in culture monolayer-expanded MSCs (volume:  $3137 \pm 213.5 \mu\text{m}^3$ ; size:  $18.06 \pm 1.4 \mu\text{m}$ , Fig 3B1) were significantly larger than the MACS-separated bioreactor MSCs expanded in parallel (volume:  $1839 \pm 95.5 \mu\text{m}^3$ ; size:  $15.1 \pm 0.9 \mu\text{m}$ ,  $p < 0.01$ , Fig. 3B2, summary in Fig. 3B3). Lastly, the mixed cell population in the bioreactors remained stable in size, while continuous passaging led to an apparent gradual increase in the cell size in monolayer cultures (Fig. 3C).

#### Improved transpulmonary transit and biodistribution of suspension-grown MSCs

The arterial MSCs concentration peaked 1 min following intravenous MSCs injection. Figure 4 shows the number of fluorescently labeled MSCs detected by flow cytometry in arterial blood samples collected at set intervals after intravenous MSCs injection in the acute *in vivo* study. The peak arterial concentration of bioreactor-expanded MSCs was significantly higher by an order of magnitude compared with rat monolayer MSCs ( $p < 0.05$ ,  $n = 6$ ). Postmortem arterial blood samples were directly plated on tissue culture plates. Twenty-four hours later, adherent MSCs-like fluorescent cells were identified from the blood of animals injected with

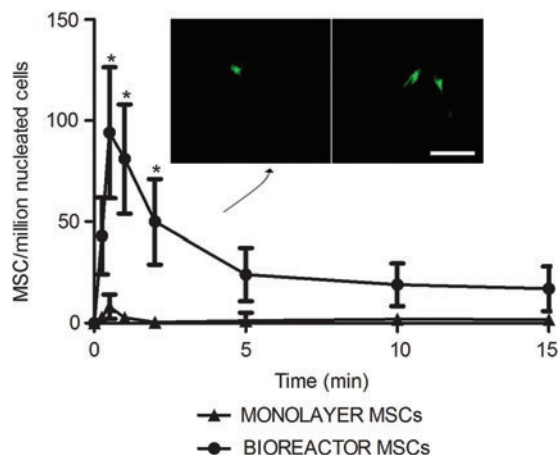


**FIG. 4.** Improved acute passage through the pulmonary microcirculation of bioreactor MSCs following intravenous injection. A significant 10-fold increase in the concentration of arterial MSCs was observed with bioreactor-expanded cells compared with the monolayer MSCs expanded in parallel following intravenous delivery in rats ( $*p < 0.01$ ). The fluorescent cell concentration was determined by flow cytometry analysis of the blood after lysis of erythrocytes. Green fluorescent cells were isolated by plating from bioreactor MSCs injected rat arterial blood, but not from the monolayer MSCs experiments (inset). Scale bar,  $100 \mu\text{m}$ . Color images available online at [www.liebertpub.com/tec](http://www.liebertpub.com/tec)

bioreactor MSCs, but not in the rats injected with monolayer-expanded rat MSCs (Fig. 4, inset).

In a different set of experiments, when the animals that were euthanized 24 h after intravenous MSC delivery, fluorescent MSCs were found predominantly in the lungs, spleens, and livers with minimal presence elsewhere (Fig. 5A). The dual labeled cells were also identified 24 h later in the lungs using X-gal staining (Fig. 5B). Because histological evaluation of cell density is difficult due to tissue autofluorescence and can be easily biased, we used a luminometry-based assay of  $\beta$ -galactosidase activity in tissue homogenates as a measure of the total content of *LacZ*-labeled MSCs in lungs, spleens, and livers (Fig. 5C, D). The  $\beta$ -galactosidase activity in the spleens and livers of rats injected with bioreactor MSCs was significantly higher than the activity in rats injected with monolayer MSCs. Compared with the lungs of rats injected with bioreactor MSCs, the lungs of rats injected with monolayer MSCs had a 3.3-fold increase in  $\beta$ -galactosidase activity (Fig. 5C,  $p < 0.01$ ,  $n = 5$ ). When  $\beta$ -galactosidase activity in the spleens or livers was normalized to that in the lungs (to correct for any differences in injection dose or cell labeling variability at the time of injection), the ratios were significantly higher in rats injected with bioreactor MSCs compared with that of rats receiving monolayer MSCs (Fig. 5D,  $p < 0.01$ ,  $n = 5$ ).

#### Discussion

Our data demonstrated that robust MSC expansion can be achieved when whole marrow combined with microbead carriers are cultured in suspension bioreactors. These culture conditions resulted in smaller MSCs with increased capacity to traverse the pulmonary microcirculation compared with conventionally expanded monolayer MSCs. This represents a potentially important attribute in optimizing the therapeutic capacity of these cells.

Traditionally, MSCs are isolated and expanded in monolayers by plating the bone marrow cells on tissue culture flasks. Uniform MSC populations can be observed after repeated passaging.<sup>13,14</sup> In an effort to preserve the bone marrow bioarchitecture, others have expanded human MSCs using whole marrow cultures in suspension bioreactors.<sup>15,17,18</sup> In these cultures, MSCs are grown in parallel with hematopoietic cell lineages, allowing for crosstalk between the stromal and other bone marrow subpopulations.<sup>15</sup> It has been proposed that, unlike traditional monolayer cultures, the bioreactor expansion approach mimics more closely the bone marrow microenvironment.<sup>15</sup> It is noteworthy that bioreactor-expanded human MSCs are highly clonogenic and have a high capacity to form colonies.<sup>17,22</sup>

We were unable to grow rat bone marrow cells in pure suspension cultures, that is, without any adhesion substrates. However, in the presence of microbead carriers, robust cell growth was obtained. The MSC content was not different in the presence of cytokine supplementation. Therefore, we used FBS as the only source of growth factors for these cells. High yield MSC expansion on similar microbead carriers has been previously demonstrated for both rat<sup>23,24</sup> and human cells.<sup>25,26</sup> Unlike these prior reports, we expanded these cultures by adding media and microbead carriers, while retaining the nonadherent cellular fractions. The rationale behind this approach is to allow for the retention of

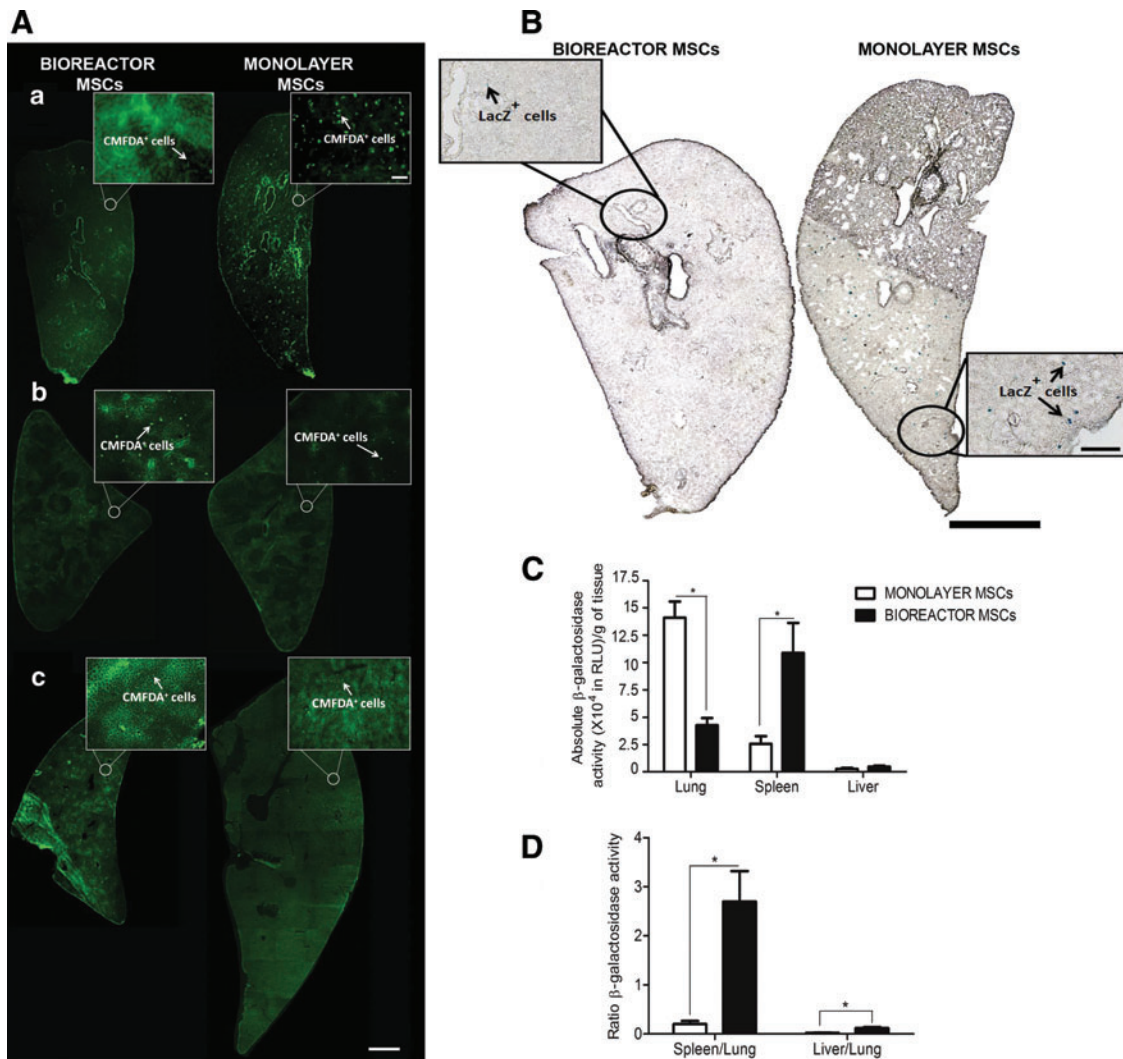


**FIG. 5.** Twenty-four hour biodistribution of MSCs following intravenous injection. Twenty-four hours after dual-labeled (CMFDA and *LacZ*) MSCs were intravenously administered, fluorescent cells were more frequent in the lungs of rats injected with monolayer MSCs compared with bioreactor MSCs (Aa). Consequently, increased number of CMFDA<sup>+</sup> cells were observed in the spleens (Ab) and livers (Ac) of rats injected with bioreactor MSCs compared with the ones receiving a bolus of the monolayer counterpart (scale bars: inserts, 100 μm; whole section reconstructions, 1 mm). The same was qualitatively noted when looking at X-gal stained tissues to identify the *LacZ*-labeled MSCs (B, scale bars: inserts, 200 μm; whole section reconstructions, 1 mm). When quantitative assessment of the number of *LacZ*-labeled MSCs was performed using whole organ measurements of β-galactosidase activity, the lungs of the bioreactor MSCs injected animals had 3.3-times less β-galactosidase activity compared with monolayer MSCs injected animals, with an inverse number observed in the spleens and livers of the later (C, \**p* < 0.05). To account for the variability of the β-galactosidase signal and the number of cells injected, the relative light unit values in the livers and spleens were normalized to the lungs in each animal; the bioreactor MSCs exhibited markedly higher spleen/lung and liver/lung ratios compared with the monolayer cells (D, \**p* < 0.01). Color images available online at [www.liebertpub.com/tec](http://www.liebertpub.com/tec)

the nonadherent MSCs, which in turn can seed new beads and are key to cell expansion using these bioreactors without actually passing the cells. Our flow cytometry and CFU data confirmed the presence of both microbead-adherent and nonadherent MSC fractions in our bioreactor cultures (Fig. 1B, D). An active interplay between nonadherent and adherent MSCs has been previously demonstrated in murine and human cells.<sup>27,28</sup> These nonadherent MSCs are dependent on the adherent fraction for their survival, and in turn have the capacity to become adherent and repopulate vacant surfaces,<sup>28</sup> a phenomenon also noted in our study with rat MSCs as well.

Bioreactor MSCs were separated at the end of the culture period by immunoselecting out the CD45<sup>+</sup> cells. These CD45<sup>-</sup> cells obtained following MACS separation (Fig. 2A) were positive for CD73, CD90, and CD105, three markers that are coexpressed on MSCs.<sup>29,30</sup> After transitioning to monolayer cultures, bioreactor cells were also able to form colonies and differentiate toward the adipogenic and osteogenic pathways (Figs. 1D and 2E–H). Together, these findings clearly indicate that an MSC population was effectively expanded in the microbead-containing bioreactors.

A key finding was that bioreactor MSCs were significantly smaller than monolayer MSCs obtained from parallel



cultures of the same duration. This was independently confirmed by both direct measurement of the cellular size on a slide using an automated cell counter and by flow cytometry. In the later method, it is also noteworthy that the CD45<sup>-</sup>/CD73<sup>+</sup>/CD90<sup>+</sup> cells present in fresh bone marrow samples (i.e., native MSCs), had a significantly lower size and FSC than cultured cells (Fig. 3A). Freshly isolated human MSCs have also been previously noted to be 10–12 μm in diameter.<sup>31</sup> Together, these are key observations underscoring the concept that the large size of cultured MSCs is a direct consequence of the culture conditions and that the native *in situ* MSCs are much smaller in size.

One of the major limitations of current systemic MSC delivery strategies is the fact that the majority of the cells become entrapped in the lung microcirculation during the first pass following intravenous administration.<sup>12,13,32</sup> Our prior data indicated that due to their increased size, monolayer-expanded MSCs are, for the most part, incapable of traversing the first pass capillary bed.<sup>11</sup> Different approaches have been proposed to circumvent this problem, including alternative culture conditions such as hanging drop aggregates<sup>19</sup> or proteolytic MSC surface modification.<sup>33</sup> Compared with monolayer MSCs, our experiments demonstrated that the smaller size of the bioreactor MSCs was indeed associated with a significantly improved capacity to traverse the lung microcirculation. Such findings were observed in both acute and chronic biodistribution studies (Figs. 4 and 5). The spleen and liver have been previously shown to function as filter/scavenger organs for intravenously injected MSCs.<sup>9,32,33</sup> In our study, compared with monolayer MSCs, there was a 3.3-fold decrease in lung β-galactosidase activity in rats injected with bioreactor MSCs 24 h postadministration (Fig. 5B, C), coincident with a higher β-galactosidase activity in the downstream spleen and liver samples (Fig. 5D). Quantitatively, our results compared favorably with other methods of improving transpulmonary transit of MSCs, such as proteolytic modification of the cell surface, where the lung retention was decreased by less than 50%.<sup>33</sup> Although we cannot eliminate the contribution of additional factors (such as different adhesion molecule profiles), the smaller size of the bioreactor MSCs is likely the main contributor to the MSCs biodistribution differences observed at this point.

In summary, our data indicate that whole-marrow bioreactor suspension cultures represent an effective method for MSC expansion. Compared with monolayer MSCs, the MSCs generated under these suspension culture conditions were smaller and had markedly increased capacity to traverse the lung microcirculation. Further work is required to evaluate whether systemic delivery of bioreactor-expanded MSCs also have greater capacity to home and to have a therapeutic effect at the organ injury site.

### Acknowledgments

This work was supported by the American Heart Association (AHA SDG grant 0835199 [PI C.T.]). Dr. Villanueva is supported, in part, by the National Institute of Health (NIH grant 5R01EB016516-02 and 5R21CA167373-02). The authors would like to acknowledge the support of the Center for Ultrasound and Molecular Imaging and Ther-

apeutics; Linda Lavery for animal care and assistance with the surgeries, and Jonathan Frank for assisting with ultrastructural imaging processing/acquisition.

### Disclosure Statement

No competing financial interests exist.

### References

- Dong, F., and Caplan, A.I. Cell transplantation as an initiator of endogenous stem cell-based tissue repair. *Curr Opin Organ Transplant* **17**, 670, 2012.
- Le Blanc, K., Frassoni, F., Ball, L., Locatelli, F., Roelofs, H., Lewis, I., Lanino, E., Sundberg, B., Bernardo, M.E., Remberger, M., Dini, G., Egeler, R.M., Bacigalupo, A., Fibbe, W., Ringdén, O., and Developmental Committee of the European Group for Blood and Marrow Transplantation. Mesenchymal stem cells for treatment of steroid-resistant, severe, acute graft-versus-host disease: a phase II study. *Lancet* **10**, 1579, 2008.
- Daly, A. Remestemcel-L, the first cellular therapy product for the treatment of graft-versus-host disease. *Drugs Today (Barc)* **48**, 773, 2012.
- Lee, J.S., Hong, J.M., Moon, G.J., Lee, P.H., Ahn, Y.H., Bang, O.Y., and STARTING Collaborators. A long-term follow-up study of intravenous autologous mesenchymal stem cell transplantation in patients with ischemic stroke. *Stem Cells* **28**, 1099, 2010.
- Hare, J.M., Traverse, J.H., Henry, T.D., Dib, N., Strumpf, R.K., Schulman, S.P., Gerstenblith, G., DeMaria, A.N., Denktas, A.E., Gammon, R.S., Hermiller, J.B., Jr., Reisman, M.A., Schaer, G.L., and Sherman, W. A randomized, double-blind, placebo-controlled, dose-escalation study of intravenous adult human mesenchymal stem cells (prochymal) after acute myocardial infarction. *J Am Coll Cardiol* **54**, 2277, 2009.
- Weiss, D.J., Casaburi, R., Flannery, R., LeRoux-Williams, M., and Tashkin, D.P. A placebo-controlled, randomized trial of mesenchymal stem cells in COPD. *Chest* **143**, 1590, 2013.
- Freyman, T., Polin, G., Osman, H., Crary, J., Lu, M., Cheng, L., Palasis, M., and Wilensky, R.L. A quantitative, randomized study evaluating three methods of mesenchymal stem cell delivery following myocardial infarction. *Eur Heart J* **27**, 1114, 2006.
- Vulliet, P.R., Greeley, M., Halloran, S.M., MacDonald, K.A., and Kittleson, M.D. Intra-coronary arterial injection of mesenchymal stromal cells and microinfarction in dogs. *Lancet* **363**, 783, 2004.
- Kraitchman, D.L., Tatsumi, M., Gilson, W.D., Ishimori, T., Kedziorek, D., Walczak, P., Segars, W.P., Chen, H.H., Fritzges, D., Izbudak, I., Young, R.G., Marcelino, M., Pittenger, M.F., Solaiyappan, M., Boston, R.C., Tsui, B.M., Wahl, R.L., and Bulte, J.W. Dynamic imaging of allogeneic mesenchymal stem cells trafficking to myocardial infarction. *Circulation* **112**, 1451, 2005.
- Schrepfer, S., Deuse, T., Reichenspurner, H., Fischbein, M.P., Robbins, R.C., and Pelletier, M.P. Stem cell transplantation: the lung barrier. *Transplant Proc* **39**, 573, 2007.
- Toma, C., Wagner, W.R., Bowry, S., Schwartz, A., and Villanueva, F. Fate of culture-expanded mesenchymal stem cells in the microvasculature: *in vivo* observations of cell kinetics. *Circ Res* **104**, 398, 2009.

12. Hoogduijn, M.J., Roemeling-van, R.M., Engela, A.U., Korevaar, S.S., Mensah, F.K., Franquesa, M., de Bruin, R.W., Betjes, M.G., Weimar, W., and Baan, C.C. Mesenchymal stem cells induce an inflammatory response after intravenous infusion. *Stem Cells Dev* **22**, 2825, 2013.
13. Caplan, A.I. Mesenchymal stem cells. *J Orthop Res* **9**, 641, 1991.
14. Pittenger, M.F., Mackay, A.M., Beck, S.C., Jaiswal, R.K., Douglas, R., Mosca, J.D., Moorman, M.A., Simonetti, D.W., Craig, S., and Marshak, D.R. Multilineage potential of adult human mesenchymal stem cells. *Science* **284**, 143, 1999.
15. Baksh, D., Davies, J.E., and Zandstra, P.W. Soluble factor cross-talk between human bone marrow-derived hematopoietic and mesenchymal cells enhances *in vitro* CFU-F and CFU-O growth and reveals heterogeneity in the mesenchymal progenitor cell compartment. *Blood* **106**, 3012, 2005.
16. Isern, J., and Méndez-Ferrer, S. Stem cell interactions in a bone marrow niche. *Curr Osteoporos Rep* **9**, 210, 2011.
17. Baksh, D., Zandstra, P.W., and Davies, J.E. A non-contact suspension culture approach to the culture of osteogenic cells derived from a CD49 subpopulation of human bone marrow-derived cells. *Biotechnol Bioeng* **98**, 1195, 2007.
18. Chen, X., Xu, H., Wan, C., McCaigue, M., and Li, G. Bioreactor expansion of human adult bone marrow-derived mesenchymal stem cells. *Stem Cells* **24**, 2052, 2006.
19. Bartosh, T.J., Ylöstalo, J.H., Mohammadipoor, A., Bazhanov, N., Coble, K., Claypool, K., Lee, R.H., Choi, H., and Prockop, D.J. Aggregation of human mesenchymal stromal cells (MSCs) into 3D spheroids enhances their anti-inflammatory properties. *Proc Natl Acad Sci U S A* **107**, 13724, 2010.
20. Zhang, Y., and Pardridge, W.M. Delivery of  $\beta$ -galactosidase to mouse brain via the blood-brain barrier transferrin receptor. *J Pharmacol Exp Ther* **313**, 1075, 2005.
21. Lennon, D., and Caplan, A. Isolation of rat marrow-derived mesenchymal stem cells. *Exp Hematol* **34**, 1606, 2006.
22. Baksh, D., Davies, J.E., and Zandstra, P.W. Adult human bone marrow-derived mesenchymal progenitor cells are capable of adhesion-independent survival and expansion. *Exp Hematol* **31**, 723, 2003.
23. Zangi, L., Rivkin, R., Kassis, I., Leviansky, L., Marx, G., and Gorodetsky, R. High-yield isolation, expansion, and differentiation of rat bone marrow-derived mesenchymal stem cells with fibrin microbeads. *Tissue Eng* **12**, 2343, 2006.
24. Yang, Y., Rossi, F.M., and Putnins, E.E. *Ex vivo* expansion of rat bone marrow mesenchymal stromal cells on microcarrier beads in spin culture. *Biomaterials* **28**, 3110, 2007.
25. Dos Santos, F., Andrade, P.Z., Abecasis, M.M., Gimble, J.M., Chase, L.G., Campbell, A.M., Boucher, S., Vemuri, M.C., Silva, C.L., and Cabral, J.M. Toward a clinical-grade expansion of mesenchymal stem cells from human sources: a microcarrier-based culture system under xeno-free conditions. *Tissue Eng Part C Methods* **17**, 1201, 2011.
26. Yuan, Y., Kallos, M.S., Hunter, C., and Sen, A. Improved expansion of human bone marrow-derived mesenchymal stem cells in microcarrier-based suspension culture. *J Tissue Eng Regen Med* **8**, 210, 2014.
27. Zhang, Z.L., Tong, J., Lu, R.N., Scutt, A.M., Goltzman, D., and Miao, D.S. Therapeutic potential of non-adherent BM-derived mesenchymal stem cells in tissue regeneration. *Bone Marrow Transplant* **43**, 69, 2003.
28. Di Maggio, N., Mehrkens, A., Papadimitropoulos, A., Schaeren, S., Heberer, M., Banfi, A., and Martin, I. Fibroblast growth factor-2 maintains a niche-dependent population of self-renewing highly potent non-adherent mesenchymal progenitors through FGFR2c. *Stem Cells* **30**, 1455, 2012.
29. Dominici, M., Le Blanc, K., Mueller, I., Slaper-Cortenback, I., Marini, F., Krause, D., Deans, R., Keating, A., Prockop, D.J., and Horwitz, E. Minimal criteria for defining multipotent mesenchymal stromal cells. The International Society for Cellular Therapy position statement. *Cytotherapy* **8**, 315, 2006.
30. Harting, M., Jimenez, F., Pati, S., Baumgartner, J., and Cox, C. Immunophenotype characterization of rat mesenchymal stromal cells. *Cytotherapy* **10**, 243, 2008.
31. Gronthos, S., Zannettino, A.C., Hay, S.J., Shi, S., Graves, S.E., Kortessidis, A., and Simmons, P.J. Molecular and cellular characterization of highly purified stromal stem cells derived from human bone marrow. *J Cell Sci* **116**, 1827, 2003.
32. Gao, J., Dennis, J.E., Muzic, R.F., Lundberg, M., and Caplan, A.I. The dynamic *in vivo* distribution of bone marrow-derived mesenchymal stem cells after infusion. *Cells Tissues Organs* **169**, 12, 2001.
33. Kerkelä, E., Hakkarainen, T., Mäkelä, T., Raki, M., Kambur, O., Kilpinen, L., Nikkilä, J., Lehtonen, S., Ritamo, I., Pernu, R., Pietilä, M., Takalo, R., Juvonen, T., Bergström, K., Kalso, E., Valmu, L., Laitinen, S., Lehenkari, P., and Nystedt, J. Transient proteolytic modification of mesenchymal stromal cells increases lung clearance rate and targeting to injured tissue. *Stem Cells Transl Med* **2**, 510, 2013.

Address correspondence to:  
 Catalin Toma, MD  
 University of Pittsburgh and  
 University of Pittsburgh Medical Center  
 966 Scaife Hall  
 3550 Terrace Street  
 Pittsburgh, PA 15218

E-mail: tomac@upmc.edu

Received: June 11, 2014

Accepted: December 8, 2014

Online Publication Date: February 26, 2015